JARQ 31, 185-193 (1997)

Optimization of the Design of Subsoiling and Pressurized Fluid Injection Equipment

Ken ARAYA

Environmental Science Laboratory, Senshu University (Bibai, Hokkaido, 079-01 Japan)

Abstract

There are 2 different design objectives for subsoilers with pressurized fluid injection, for use as pan-breakers or injectors, respectively. A large soil failure is desirable when a subsoiler is used as a pan-breaker and minimal soil failure is preferable when it is used as an injector. This paper determines the optimum shapes of a pan-breaker and injector, where the draught can be reduced by injecting pressurized air (about 1.2 MPa at the air tank) from a nozzle port at the tip of the chisel. The results show that the optimum pan-breaker with fluid injection should have a rake angle of 45 to 60°, a chisel thickness of 50 × 50 mm, and a heel position at 100 mm. The optimum injector with fluid injection should have a rake angle of 90°, a shank thickness of less than 15 mm, a chisel length of 250 mm, a chisel thickness of 30 × 30 mm, and a heel position at 100 mm.

Discipline: Agricultural machinery
Additional key words: subsoiler, injector, draught

Introduction

There are 2 design objectives for the subsoiler with pressurized fluid injection, which is being developed by the author. One is for use as a pan-breaker which improves heavy clay soils[1,2,5] and the other as an injector for the placement of liquid fertilizer under pressure in asparagus rhizosphere[8]. Extensive soil failure is desirable for the pan-breakers and minimal soil failure for the injectors, to avoid cutting roots.

The specific objectives were: (1) to optimize the design of tillage tools to minimize the energy used in soil disturbance, (2) to optimize the use of pressurized air or liquid to reduce the draught requirements of implements.

Basic tests were conducted with air injection in a movable soil bin which can be handled easily in the laboratory. It was assumed that the prototype subsoiler would inject viscous liquid organic matter such as sewage sludge[6]. The differences in soil failure between air injection and viscous liquid injection have been reported elsewhere[3,7].

This paper first deals with the relation between soil failure rates and the shape of shanks and chisels without fluid injection and then with the shape of pan-breakers and injectors, where the draught was reduced by the injection of pressurized air (about 1.2 MPa at an air tank) from a nozzle port at the tip of the chisel, after modification of the shapes of the subsoiler without fluid injection.

Methods

Laboratory subsoiler tests were conducted in a movable soil bin (53 cm high, 180 cm long, 50 cm wide) shown in Fig. 1, sufficiently large for testing the prototype subsoiler. A soil bin speed of 16 mm/s was used for all the tests. This speed was low compared with the subsoiler operation in the field, but the capacity of the soil bin drive system was limited to this speed. Stafford[10] reported variations in the speed of simple blades, from 5 mm/s to 5 m/s and did not detect any difference in the rupture area in clay soils and generally no correlation between speed and rupture area. The depth of tillage could be controlled by an elevating device on the frame. In the present experiments, the operational depth of the subsoiler was 30 cm.

Air was compressed in an air cylinder with a compressor. Control valve A (Fig. 1) released air at a specified flow rate through the high pressure rubber hose to the nozzle port of the subsoiler. When air

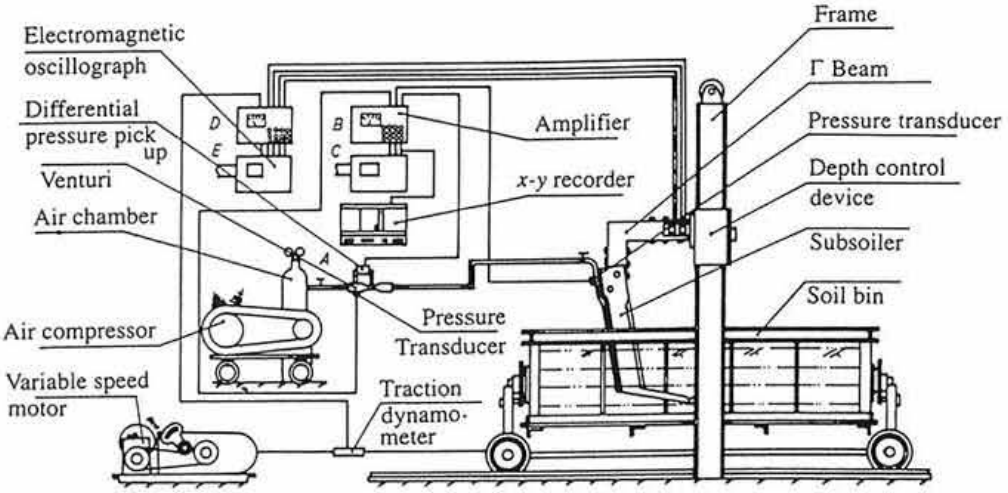

Fig. 1. Model test apparatus
The soil bin is 1,808 mm long, has a transparent side and is propelled by a variable speed motor.

was introduced into soil from the nozzle port, the air pressure associated with air resistance through the soil was produced at the nozzle port. This air pressure was measured with a pressure transducer on the shank and was recorded with an electromagnetic oscillograph C through the amplifier B. Air flow rate was measured by sensing the difference of pressure of the venturi (Fig. 1) with a differential pressure transducer. This pressure difference was recorded in the Y direction of the X–Y recorder through the amplifier B. The horizontal (x) force (draught), vertical (z) force and moments on the tine (Fig. 2) could be measured by the Γ beam[4] (Fig. 1) and the draught was verified by using a traction dynamometer between the soil bin and the variable speed motor. Four output signals from the Γ beam and 1 output signal from the traction dynamometer, were recorded on the electromagnetic oscillograph E through the amplifier D. The fluid flow rate, the pressure at the venturi, and the air pressure produced at the nozzle port, were recorded on the electromagnetic oscillograph C through the amplifier B.

The soil in this study consisted of sand (liquid limit = plastic limit = non-plastic, moisture content 9.5% d.b.), and the values of the soil-interface friction and soil-metal friction angles are shown in Table 1. The 40 cm deep soil was prepared by compacting 10 cm layers to a hardness of 10 mm on Yamanaka's hardness tester scale.

The subsoilers consisted of fabricated shanks and chisels as shown in Fig. 2(b) and compared with conventional subsoilers, they had a long chisel and a nozzle port at the tip of the chisel. To prevent air leakage, a wedge type plug (hereafter designated as heel) as shown in Fig. 2(b) was developed.

Definition of rupture power

The schematic diagrams of soil failures are shown in Fig. 2. Fig. 2(a) shows the soil failure induced by a shank without a chisel. Godwin and Spoor[4] developed a force prediction model for such narrow tines and indicated the critical depth of a tine below which the soil failure mechanism changed. The working depth/width ratio, that is the aspect ratio, of the subsoiler shank in this study showed a minimum value of 6 (300 mm/50 mm) and there was a crescent failure with a distinct slip surface developed from the shank base and lateral failure below the critical depth (point M in Fig. 2(a)) without the

Table 1. Mechanical properties of soil in this study

	Soil moisture (w, %d.b.)	Wet bulk density (ρ, kg/cm^3)	Angle of soil-interface friction (ϕ, °)	Cohesion (c, MPa)	Adhesion (c', MPa)	Angle of soil-metal friction (δ, °)
Sand	9.5	1,430	23.8	0.009	0	15.0

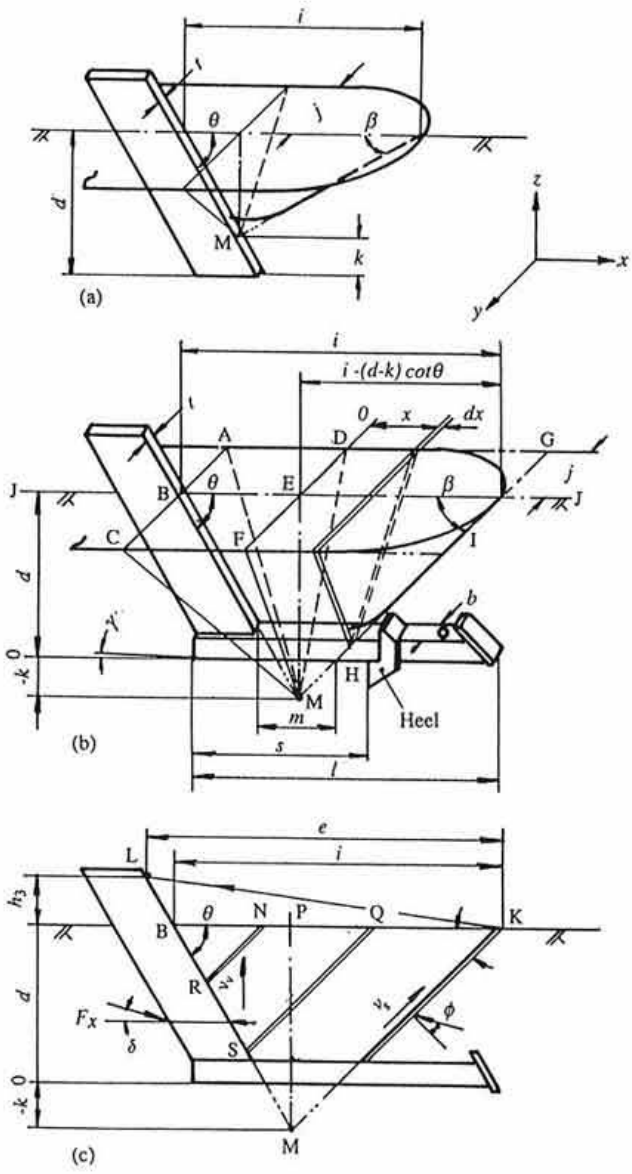

Fig. 2. Schematic diagram of soil failure
(a) Soil failure induced by shank without chisel.
(b) Soil failure induced by shank with chisel.
(c) Section J-J of (b).

formation of a distinct slip surface.

Fig. 2(b) shows the soil failure induced by a shank with a chisel. There was no lateral failure and the starting point of the slip surface moved to the center (point H in Fig. 2(b)) of the chisel.

The author defined the soil rupture power W_s as:

$$W_s = W_{s1} + W_{s2} \quad \text{..... (1)}$$

where W_{s1} is the power to move soil vertically, and W_{s2} is the power to disturb soil.

W_{s1} can be obtained as:

$$W_{s1} = \frac{vS\rho gh_3}{3} + (F_x \tan\delta)\frac{v}{3} \quad \text{..... (2)}$$

where F_x is the horizontal force (draught), N, S is the disturbed area (yz plane), m^2, g is the acceleration of gravity, m/s^2, h_3 is the maximum vertical soil movement at the soil surface, m, v is the subsoiler speed, m/s, δ is the angle of soil-metal friction, deg. and ρ is the soil bulk density, kg/m^3.

W_{s2} can now be obtained as:

$$W_{s2} = \frac{vh_3}{3e\sin\beta}\left[c\sum_{k=1}^{n} S_k + \tan\phi\cos\beta\sum_{k=1}^{n} W_k\right]$$

$$= \frac{vh_3}{3e\sin\beta}$$

$$\left[cS_1\left\{1 + \frac{(n-1)^2}{n^2} + \frac{(n-2)^2}{n^2} + \cdots\right\}\right.$$

$$+ \tan\phi\cos\beta$$

$$\left.W_1\left\{1 + \frac{(n-1)^3}{n^3} + \frac{(n-2)^3}{n^3} + \cdots\right\}\right]$$

$$\text{..... (3)}$$

where c is the soil-interface adhesion, Pa, e is the distance of soil movement, m, n is the number of slip surfaces, β is the angle of slip surface, deg and ϕ is the angle of soil-interface friction, deg.

Results and discussion

1) Effect of heel

The resulting soil failure with air injection is shown in Plate 1, i.e. a cavity behind the nozzle port caused by air injection. In Plate 1(a), the rake angle θ was 60°, shank thickness 15 mm, chisel length 450 mm, and chisel thickness 30 × 30 mm. When the subsoiler was inclined and the chisel angle γ (see Fig. 2(b)) increased, the air injected from the nozzle port leaked to the subsoiler path without soil break-up and no draught reduction was obtained as shown in Fig. 3(a). When the γ value was 13° in Fig. 3(a), there was no draught reduction. When the value of the chisel γ angle ranged from 3 to 8° as in Fig. 3(a), the heel showed a resistance and F_x increased above that without heel. The vertical force F_z became negative at $\gamma = 3°$ and the so-called suction did not work as evidenced when air was injected. If subsoilers do not have a suction mechanism, they cannot be used in practice. The optimum shape of a heel with small F_x and a positive F_z still remains to be

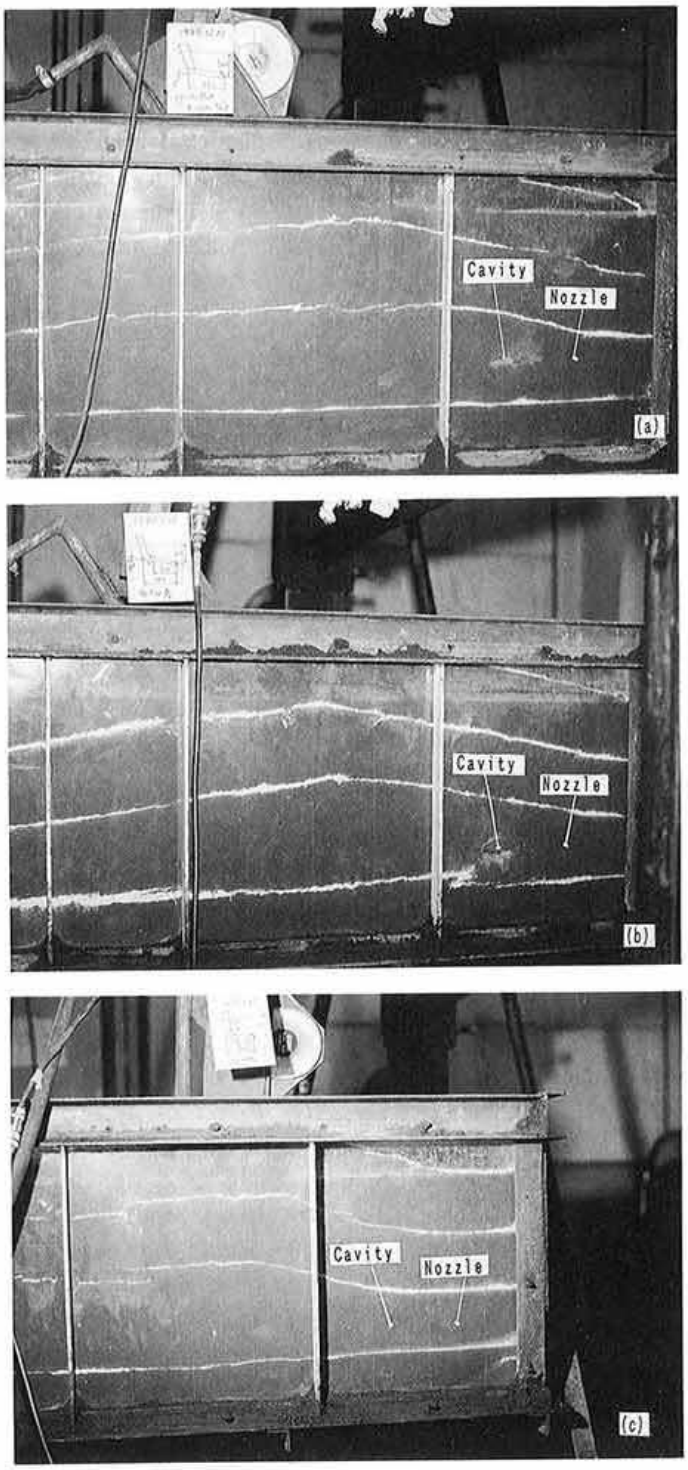

Plate 1. Soil failure induced by different subsoilers injecting air at 25 g/s in sand with 9.58% d.b. soil moisture
(a) Rake angle $\theta = 60°$, shank thickness $t = 15$ mm, chisel length $l = 450$ mm, chisel thickness $b = 30 \times 30$ mm.
(b) Rake angle $\theta = 60°$, shank thickness $t = 15$ mm, chisel length $l = 450$ mm, chisel thickness $b = 50 \times 50$ mm, heel position $s = 100$ mm.
(c) Rake angle $\theta = 90°$, shank thickness $t = 13$ mm, chisel length $l = 250$ mm, chisel thickness $b = 30 \times 30$ mm, heel position $s = 100$ mm.

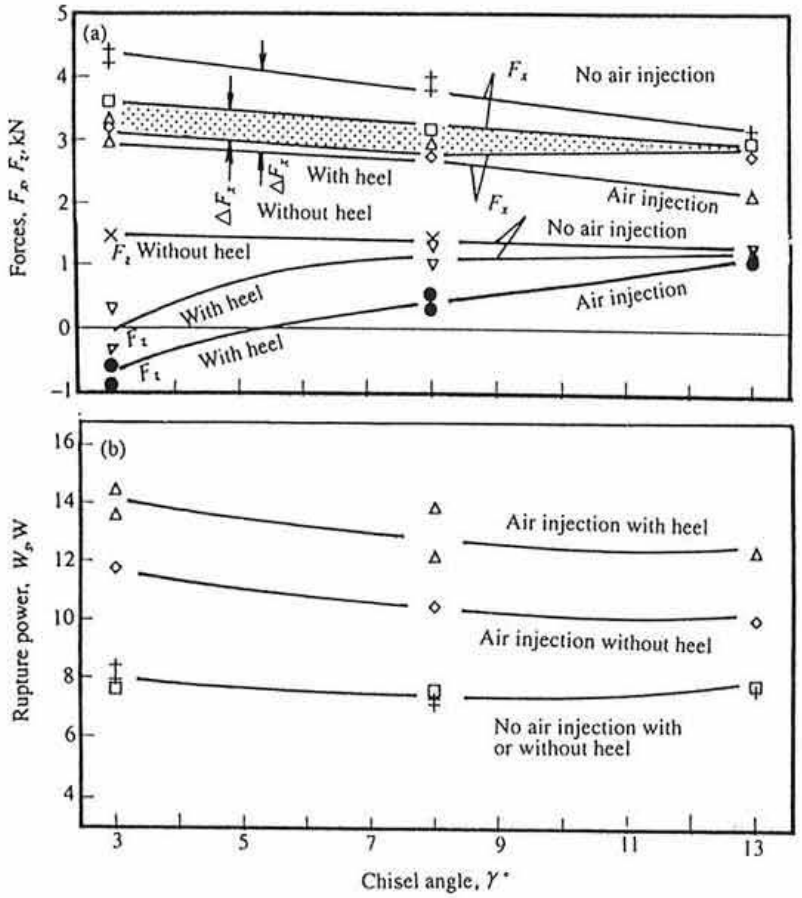

Fig. 3. Horizontal and vertical forces and rupture power as a function of chisel angle
Rake angle $\theta = 60°$, shank thickness $t = 15$ mm, chisel length $l = 450$ mm, heel position $s = 100$ mm, with and without heel.

determined. However, when the heel was set as in Fig. 3(a), draught reduction was obtained even at larger γ value. When the heel was set as in Fig. 3(b), soil failure by the air injection increased and the rupture power W_s also increased.

In Fig. 3(b), the total W_s was about 13.5 W, with the power to move soil vertically W_{s1} 2.5 W based on Eq. 2 and the power to disturb soil W_{s2}, 11 W. In W_{s1}, the power to move soil vertically only (first term of Eq. 2) was about 1.5 W and the friction acting on the shank (second term of Eq. 2) was about 1.0 W. In W_{s2}, the shear (first term of Eq. 3) was 10.5 W and the internal friction (second term of Eq. 3) was 0.5 W. Consequently, almost all of the power was consumed by shear.

2) Appropriate position of heel

The results with different heel positions are shown in Fig. 4, where the chisel length was 450 mm. In Fig. 4(a), when the heel was set at $s = 300$ mm, near the nozzle port, F_x increased because the heel created a resistance. Draught reduction by air injection ΔF_x was not affected by the heel position. In Fig. 4(b), the rupture power W_s reached a maximum value when the heel was at 100 mm. Consequently, the optimum heel position was 100 mm, closest to the shank, because of the lower resistance.

3) Appropriate length of chisel

To determine the appropriate dimension for pan-breakers, the rake angle should be 60° and therefore, soil failure was investigated by varying the chisel length to 250, 350, and 450 mm (the results are shown in Fig. 5). In Fig. 5(a), the forward rupture distance i increased in proportion to the chisel length and the sideways rupture distance j was constant at 300 mm, regardless of the chisel length. The rupture distances of i and j did not change by air

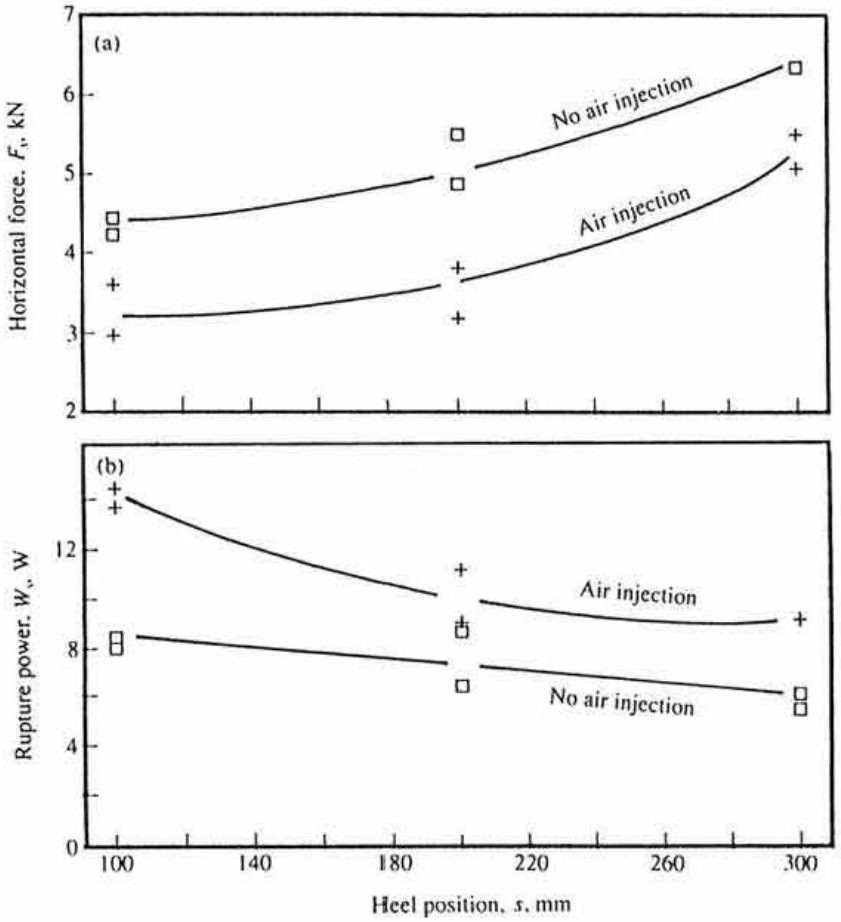

Fig. 4. Horizontal force and rupture power as a function of heel position
Rake angle $\theta = 60°$, shank thickness $t = 15$ mm, chisel thickness $b = 30 \times 30$ mm, chisel length $l = 450$ mm, chisel angle $\gamma = 3°$.

injection.

In Fig. 5(b), a draught reduction ΔF_x of 1,500 N was obtained by air injection. In Fig. 5(c), the rupture power W_s increased from 10 to 13 W by air injection. The air injection did not induce changes on the soil surface but a cavity was formed around the nozzle port and the soil was disturbed. In Fig. 5(d), the disturbance efficiency W_s/W_f increased in proportion to the chisel length with air injection. The rupture power W_s increased with longer chisels and the chisel length should be as long as strength permits as the injected air does not leak to the subsoiler path but effectively breaks the soil.

To determine the appropriate dimensions for injectors, the rake angle θ was set at 90° and the chisel length measured 130, 200, 250, or 450 mm. Chisel length below 250 mm, was used to further decrease the rupture power W_s, and the results are shown in Fig. 6. In Fig. 6(a), both rupture distances i and j were smaller than those in Fig. 6 when the rake angle was 60°.

In Fig. 6(b), the draught F_x decreased when the chisel length ranged from 250 to 450 mm with air injection but did not decrease below 250 mm. Consequently, when the chisel used was too short, the injected air leaked to the subsoiler path and did not break the soil.

In Fig. 6(c), the rupture power W_s increased by air injection at chisel lengths above 250 mm. In Fig. 6(d), the disturbance efficiency also increased at chisel lengths above 250 mm. Consequently, the optimum chisel length of the injectors was 250 mm, ensuring that the rupture power was not large and that draught reduction was obtained by air injection.

4) Optimum shapes of pan-breaker and injector with air injection

Table 2 shows the optimum dimensions of pan-breakers and injectors with air injection based on the results of Figs. 5 and 6. Plate 2(a) shows a pan-breaker with the dimensions indicated in Table 2. Soil failure by this pan-breaker is shown

in Plate 1(b).

An injector with the dimensions indicated in Table 2 is shown in Plate 2(b). Soil failure induced by this injector is depicted in Plate 1(c). The rupture distance and soil movement were much smaller than those of the pan-breaker depicted in Plate 1(b).

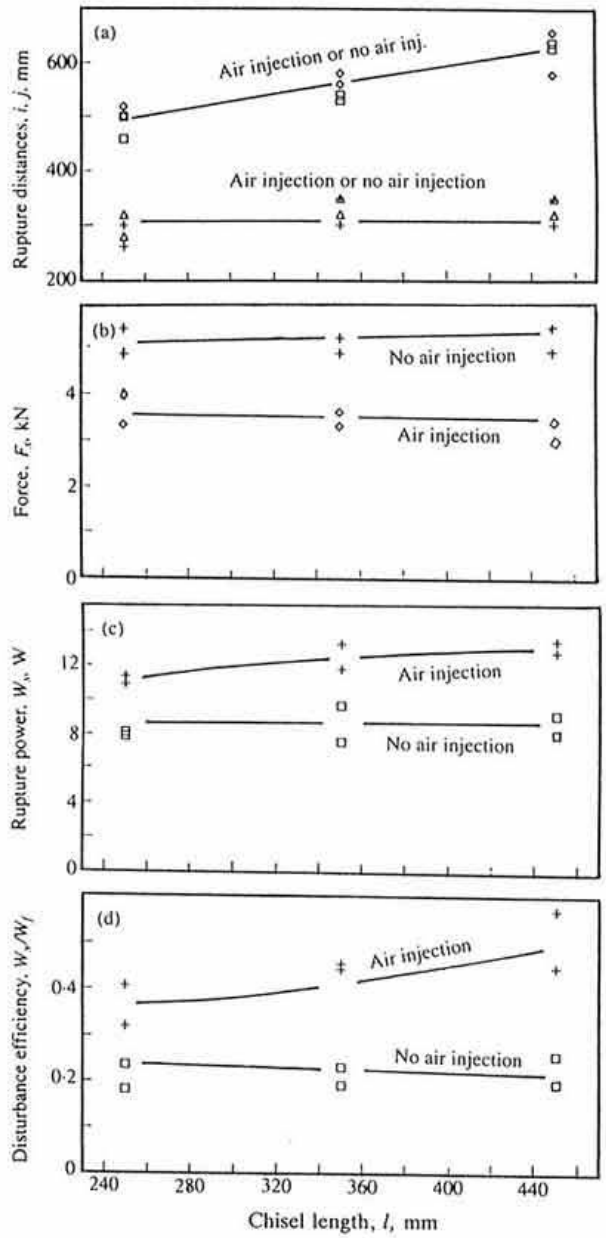

Fig. 5. Rupture distance, force, rupture power, and disturbance efficiency as a function of chisel length
Rake angle $\theta = 60°$, shank thickness $t = 15$ mm, chisel thickness $b = 30 \times 30$ mm, chisel angle $\gamma = 3°$, heel position $s = 100$ mm.

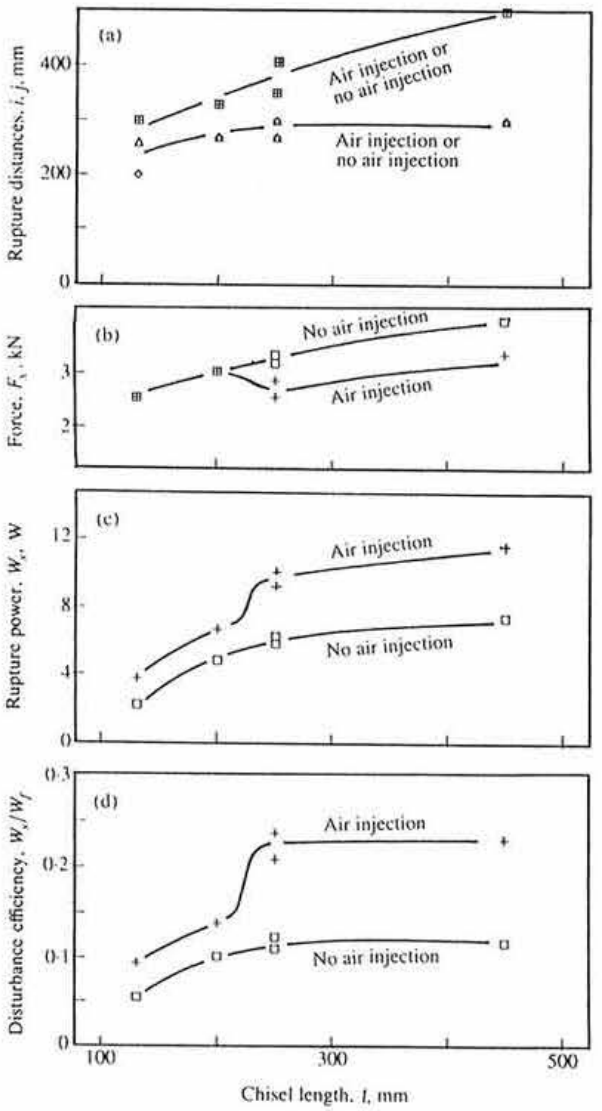

Fig. 6. Rupture distance, force, rupture power, and disturbance efficiency as a function of chisel length
Rake angle $\theta = 90°$, shank thickness $t = 15$ mm, chisel thickness $b = 30 \times 30$ mm, chisel angle $\gamma = 3°$, heel position $s = 100$ mm.

Table 2. Optimum dimension of pan-breaker and injector with fluid injection

	Rake angle (θ, °)	Shank thickness (t, mm)	Chisel length (l, mm)	Chisel thickness (b, mm)	Heel position (s, mm)
Pan-breaker	45 - 60	more than 15	450	50 × 50	100
Injector	90	less than 15	250	30 × 30	100

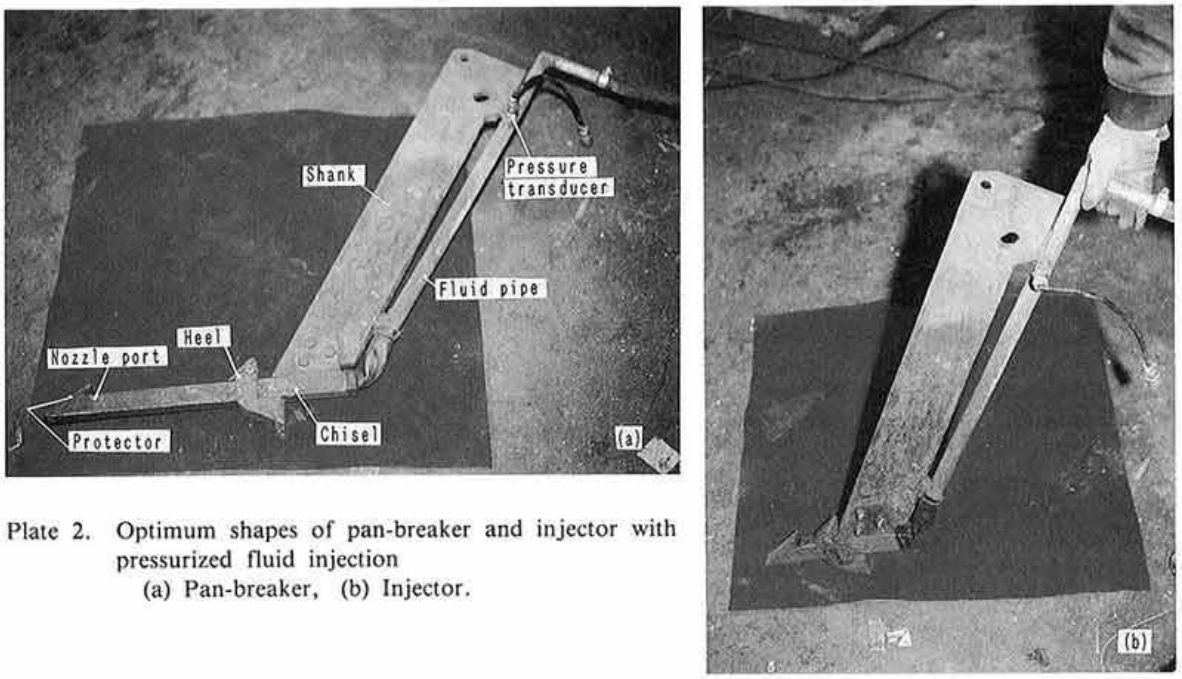

Plate 2. Optimum shapes of pan-breaker and injector with pressurized fluid injection
(a) Pan-breaker, (b) Injector.

Conclusion

1. The pan-breakers should have a rake angle of 45 to 60° for a maximum rupture power and efficiency and the injectors should have a rake angle of 90° to achieve a minimum rupture power and draught.
2. The injectors for small soil failure rates should have shank thicknesses of less than 15 mm and the appropriate breakers should have shank thicknesses of 15 to 50 mm.
3. With injectors, short chisel lengths are preferable because of the smaller rupture power.
4. The rupture power increased with chisel thickness because a thicker chisel gave rise to more soil failures, and a thicker chisel is recommended for pan-breakers.
5. When the subsoiler was inclined and the value of the chisel angle γ increased, the air injected from the nozzle port leaked to the subsoiler path without soil break-up and no draught reduction was obtained. To prevent the air leakage, a wedge type plug, i.e. heel was developed. The optimum heel position was 100 mm, closest to the shank, because of the lower resistance.
6. In pan-breakers, the rupture power increased with longer chisels and the chisel length should be as long as strength permits as the injected air does not leak to the subsoiler path but effectively breaks the soil.
7. In injectors, the optimum chisel length was 250 mm, ensuring that the rupture power is not large and that draught reduction is obtained by air injection.

References

1) Araya, K. & Kawanishi, K. (1981): Pressure produced when fluid is introduced under pressure into soil-bed layer (Part 1). *J. JSAM*, **43**(1), 19-29 [In Japanese with English summary].
2) Araya, K., Kawanishi, K. & Gao, R. (1982): Pressure produced when fluid is introduced under pressure into soil-bed layer (Part 4). *J. JSAM*, **44**(2), 281-292 [In Japanese with English summary].
3) Araya, K. (1982): Soil failure by introducing fluid under pressure. *J. Senshu Univ.-Hokkaido*, **15**, 1-85.
4) Araya, K. (1983): Soil failure by introducing fluid under pressure (I). *J. JSAM*, **45**(1), 35-41 [In Japanese with English summary].
5) Araya, K. & Kawanishi, K. (1984): Soil failure by introducing air under pressure. *Trans. ASAE*, **27**(5), 1292-1297.
6) Araya, K. (1985): Soil failure by introducing sewage sludge under pressure. *Trans. ASAE*, **28**(2), 397-400, 404.
7) Araya, K. (1985): Soil failure by introducing fluid under pressure. *In* Proc. Int. Conf. Soil Dynamics, Auburn University, USA.
8) Araya, K. et al. (1990): An injector of pressurized liquid fertilizer into asparagus rhizoshere (Part 1). *J. JSAM*, **52**(4), 61-66 [In Japanese with English

summary].
9) Godwin, R. J. & Spoor, G. (1979): Soil failure with narrow tines. *J. Agric. Eng. Res.*, **22**, 213–228.
10) Stafford, J. V. (1979): The performance of a rigid tine in relation to soil properties and speed. *J. Agric. Eng. Res.*, **24**, 41–56.

(Received for publication, December 16, 1996)